JOURNAL OF SOLID STATE CHEMISTRY 91, 350–361 (1991)

X-Ray and Neutron Diffraction Studies of the Diffuse Phase Transition in $PbMg_{1/3}Nb_{2/3}O_3$ Ceramics

P. BONNEAU, P. GARNIER, AND G. CALVARIN

Laboratoire de Chimie-Physique du Solide, URA CNRS 453, Ecole Centrale de Paris, 92295 Chatenay-Malabry Cedex, France

E. HUSSON*

E.S.E.M. Université d'Orléans CRPHT-CNRS 45045 Orléans Cedex, France

J. R. GAVARRI

Université de Toulon et du Var, LCMPCT, B.P. 132, 83957, La Garde, France

A. W. HEWAT

Institute Laue-Langevin, Avenue des Martyrs, 156X, 38042 Grenoble Cedex, France

AND A. MORELL

Thomson-CSF, LCR, Domaine de Corbeville, 91404 Orsay Cedex, France

Received October 1, 1990

X-ray and neutron diffraction patterns of lead magnesium niobate (PMN) were recorded between 800 and 5 K. The evolution of the cubic cell parameter and of the thermal expansion coefficient was analyzed and structural refinements were carried out by the Rietveld method. In the cubic phase of space group *Pm3m* the atoms exhibit important shifts from their special positions. A disordered structural model leading to a discrepancy factor $R_{wp} = 7.21\%$ is proposed. The nucleation of polar microregions begins at 600 K; it is revealed on the X-ray and neutron diffraction patterns only by some line tails which increase when the temperature is lowered. A structural refinement at 5 K leads to a R_{wp} factor of about 11%. Therefore this model has to be improved in order to take into account the existence of polar microregions with very small correlation lengths.

Introduction

Lead magnesium niobate $PbMg_{1/3}Nb_{2/3}O_3$ (PMN) is one of the most interesting perovskite relaxors. The high temperature phase is cubic with space group *Pm3m*, whereas below 200 K a small rhombohedral distortion was observed by Shebanov (*1*) from single crystal studies. The ferroelectric phase transition is very diffuse and occurs in a temperature range of several tens

* To whom correspondence should be addressed.

0022-4596/91 $3.00

of degrees. In a recent paper (*2*), we studied the mean cubic structure of PMN ceramics by X ray diffraction between 297 and 1023 K. Structural refinements from integrated peak intensities have shown that Pb and Nb atoms are statistically shifted off the special positions of the ideal cubic perovskite structure. We have completed this work by:

(i) a neutron diffraction study between 297 and 800 K in order to determine precisely the positions of the oxygen atoms in the high temperature phase;

(ii) a neutron and X-ray diffraction coupled study between 297 and 5 K in order to find the ferroelectric transition and the ferroelectric phase.

Experimental

PMN ceramics have been prepared according to the process described in (*3*) and the samples used for this study were powders obtained by crushing sintered ceramic disks and annealed in order to reduce the grinding effects.

The X-ray powder patterns were recorded over the angular range $10 < 2\theta < 130°$ on a high-accuracy diffractometer MICROCONTROLE using Cu$K\alpha$ radiation (graphite monochromator) of a rotating anode generator of 18 kW. The low temperature study has been performed in a MERIC cryostat with a stability and a precision of 0.1 K. In order to avoid the orientation effects, different samples have been analyzed.

The neutron powder diffraction patterns were collected on the D1A and D2B diffractometers attached to the I.L.L. in Grenoble, over the angular range $10 < 2\theta < 160°$ by steps of 0.05° (2θ). The wavelengths used were 1.384 Å on D1A and 1.595 Å on D2B. The PMN powder was put in a vanadium can.

The structural refinements were carried out using the profile Rietveld method (*4*) by means of the computer program DBW3.2 (*5*).

Evolution of the Diffraction Patterns with Temperature

X-ray Powder Patterns

Above and at 297 K, as already reported (*2*), a classical pattern of a ABO_3 cubic perovskite is obtained with the quasi-extinction of some reflection lines i.e. (320), (322)–(410), (331), (421). There is no evolution in the profile of the diffraction lines except a slight increase of about 9% of the full width at half-maximum (FWHM) with decreasing temperature.

Below 297 K and down to 5 K no splitting of the lines or shoulders, indicating a distortion of the cubic cell, is observed: the FWHM increase continuously of about 19% for all the lines. This result is not coherent with a tetragonal, orthorhombic, or rhombohedral distortion. This change in lineshape could result from the growth of the polarized regions, like in PLZT (*6*). Therefore, a careful analysis reveals:

(i) the progressive appearance of the quasi-extincted lines of the high temperature phase in the form of very large (about 1.5° 2θ FWHM) weak lines (see Fig. 1);

(ii) a slight widening of the basis of some lines especially for the reflections with indices of different parities (see Fig. 2).

Neutron Powder Patterns

The evolution of the powder patterns between 800 and 5 K is the same as that for the X-ray diffraction. Two main features are observed on the diffraction profiles:

(i) a modulated background which increases between 800 and 300 K and remains quite constant below 300 K. This important scattering intensity, shown in Fig. 3, reveals correlations in the nature or in the positions of atoms and could be explained either by the existence of nanodomains in

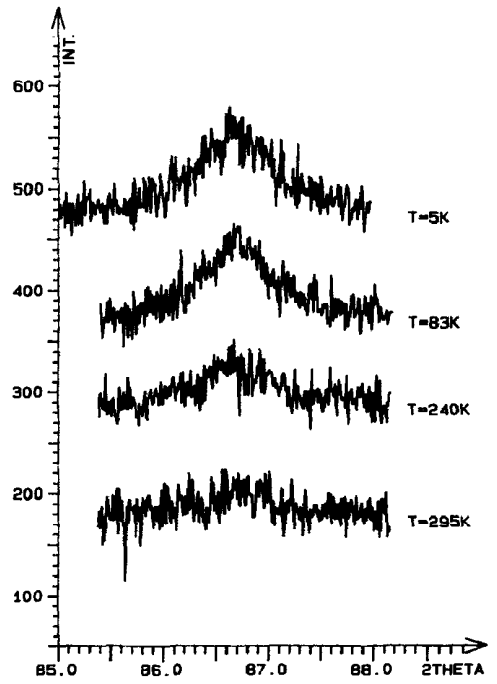

FIG. 1. Progressive appearance of the (320) line on the X-ray diffraction patterns with decreasing temperature.

which the Mg^{2+} and Nb^{5+} cations are 1-1 ordered on the *B* site of the perovskite structure (this ordering has been pointed out by electron diffraction and high resolution transmission electron microscopy (*7, 8*)) or by a precursor effect of the ferroelectric phase transition.

(ii) the existence of tails for some lines more important than those on the X-ray diffraction patterns: the lines for which all three indices have the same parity exhibit the same profile from 800 to 5 K whereas the lines with different parity indices exhibit an important widening at their bases, particularly those with two odd indices. Figure 4 shows the evolution of some line tails with temperature between 800 and 5 K: the widening begins at high temperature, around 600 K, increasing continuously down to 5 K and this effect is maximum between 400 and 300 K.

Evolution of the Cell Parameter and Thermal Expansion

Figure 5a shows the variation of the cubic cell parameter, a_c, determined at different temperatures by least square refinement using 22 reflections, and of the thermal expansion coefficient α. The curve $a_c = f(T)$ is linear at high temperature and exhibits a slope modification around 600 K. Below 300 K, a_c remains roughly constant. The thermal expansion coefficient is constant above 610 K and it is equal to 10×10^{-6} K^{-1}, a value generally found in other perovskite oxides (*9*). But, below 290 K, α becomes abnormaly weak and lower than

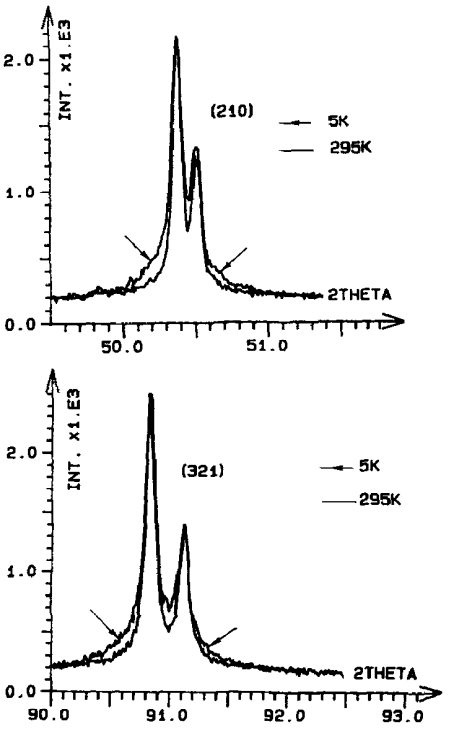

FIG. 2. Line tails observed at low temperature on the X-ray diffraction patterns.

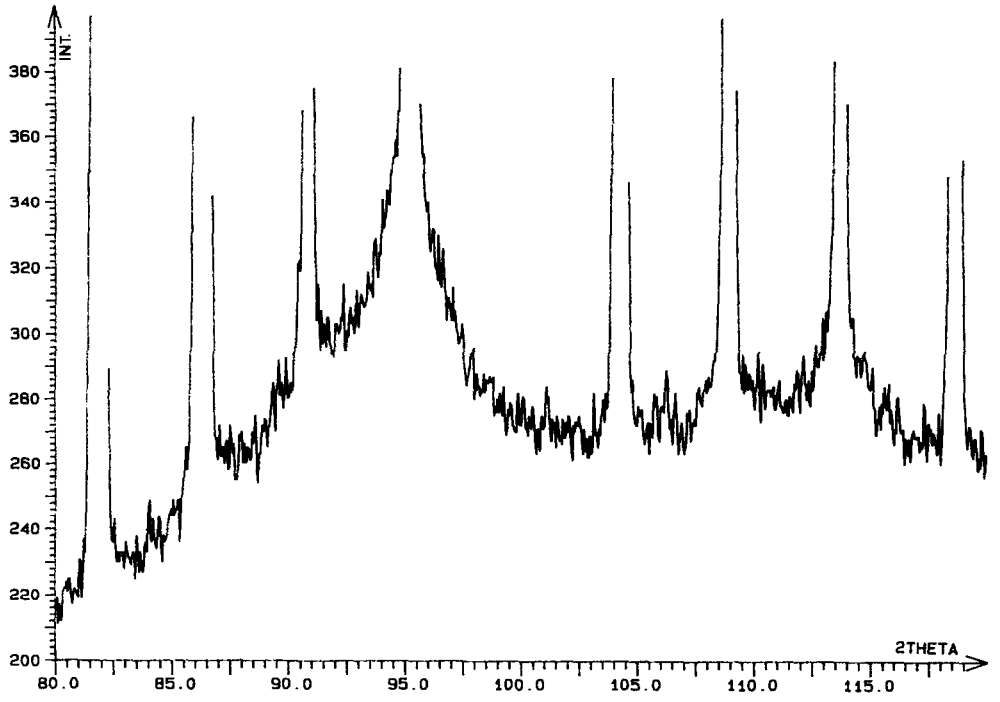

FIG. 3. Modulated background observed at 307 K on the neutron diffraction pattern.

1.10^{-6} K^{-1}. A noticeable jump of a_c or α around 200 K as observed by Shebanov was not seen (*1*). However, our results are in excellent agreement with the dilatometric study reported by Cross (*10*) who observes that the rate of thermal strains S_{11} of PMN ceramic is found to continuously decrease below 610 K, as is shown in Fig. 5b. The author attributes this reduction to the electrostrictive consequence of an increasing root mean square polarization $\sqrt{P^2}$ below this temperature. The identical thermal behavior of the PMN at the macroscopic and microscopic levels seems to confirm this assumption.

Refinement of the Structure

Preliminary Considerations

Taking into account the disordered positions of atoms pointed out in the previous structural study (*2*) and the limited number of reflections (the Bragg peaks were observed up to the 440 reflection) the atomic displacements and the thermal parameters B cannot be easily separated in the structural refinement calculations. Then, the B values found at various temperatures for other perovskite compounds, similar to PMN, i.e., $PbTiO_3$ (11, 12) and $BaTiO_3$ (13), have been used. So, the isotropic B parameters have been fixed for all the calculations. The refined parameters were: an overall scale factor, three profile parameters, the counter zero error, and the atomic positions. The background was measured on each pattern out of Bragg peaks, and it was interpolated between these values.

The preliminary refinement has been performed with the neutron diffraction data at 307 K, in the same way as for the X-ray diffraction data. When all atoms are fixed on their special positions in the space group

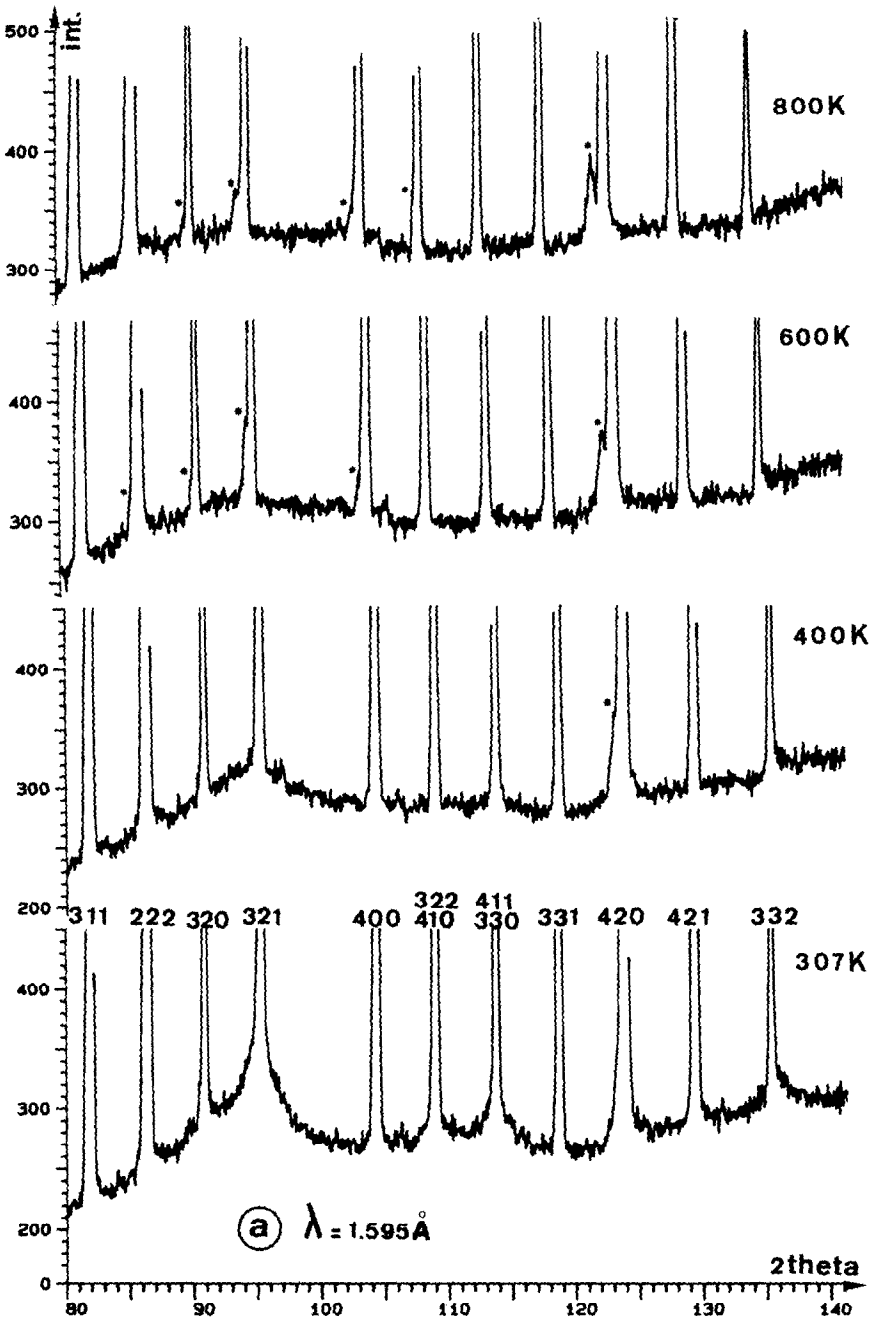

FIG. 4. Evolution of some neutron diffraction lines between 800 and 5 K. (a) Diffraction patterns recorded on D2B. (b) Diffraction patterns recorded on D1A.* Parasite lines due to an oxygen-deficient phase of PMN formed at high temperature.

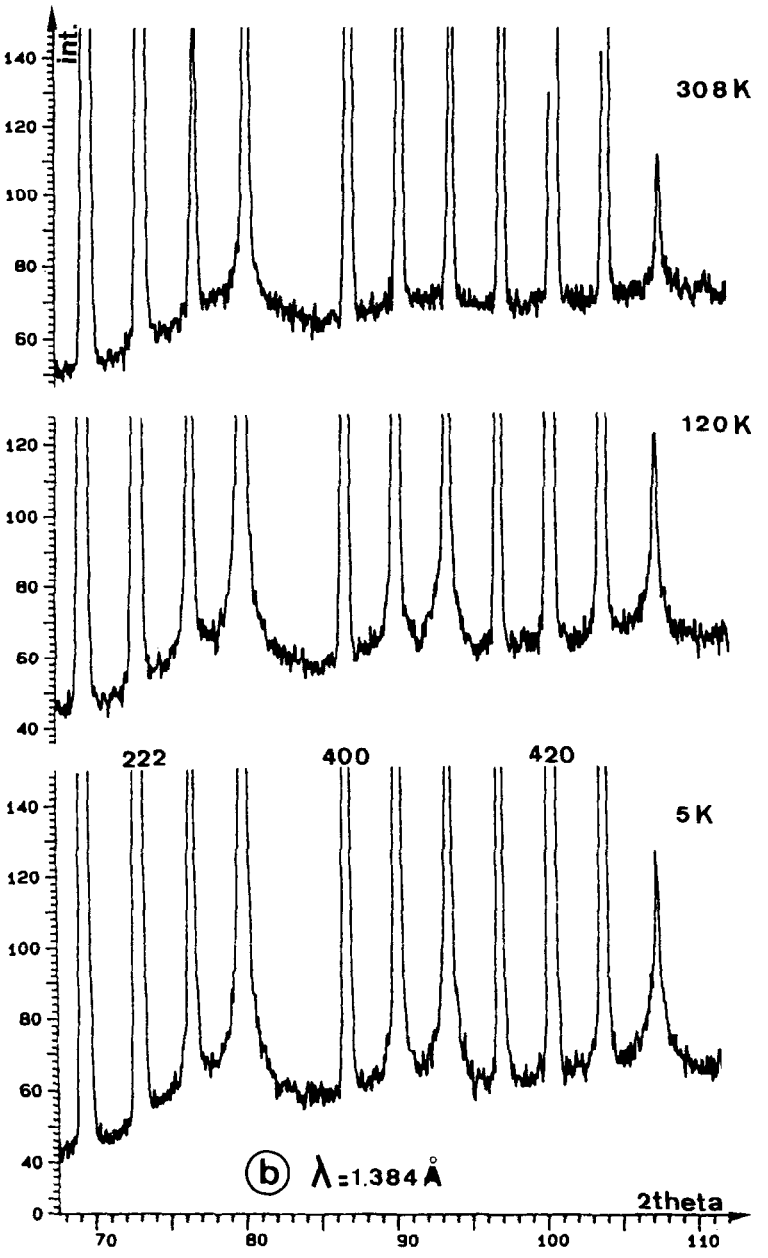

$Pm3m$, the R_{wp} factor is about 31.7%. The refinement of the B factor of Pb atoms leads to a very high value of 3.8 $Å^2$, which confirms displacements of these atoms.

The displacements of Pb atoms from their special positions along the ⟨100⟩, ⟨110⟩, or ⟨111⟩ directions have been considered. Atomic positions are fixed step by step along these directions and the corresponding R_{wp} factors are calculated. The

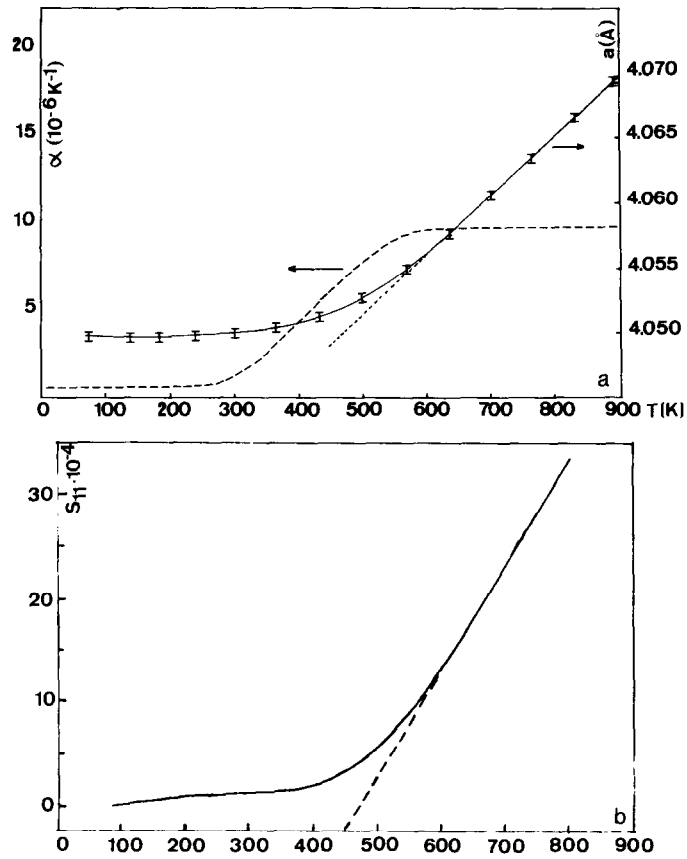

FIG. 5. (a) Evolution of the cubic cell parameter and of thermal expansion $\alpha = 1/L \cdot (\Delta L/\Delta T)$ vs temperature. (b) Thermal strain $S_{11} = \Delta L/L$ vs temperature for PMN according to (*10*).

minimum value of $R_{wp} = 17.9\%$ is obtained for atomic shifts of 0.32 Å along the ⟨110⟩ or ⟨111⟩ directions. The shifts of oxygen atoms are then determined in the same manner. For the O atom in the *xy* plane (*C* face), shifts along the nonequivalent [100] and [001] directions and along the [110] and [111] directions are considered. The minimum value of $R_{wp} = 10.8\%$ is obtained for shifts of 0.17 Å along the [100] and [110] directions and of 0.08 Å along the [001] direction. So, it can be assumed that oxygen atom is isotropically distributed on two parallel rings about 0.08 Å distant from the *xy* plane; identical configurations can be proposed for the oxygen atoms lying in the *A* and *B* faces. Finally, the displacements of Nb/Mg atoms have been considered. Shifts of about 0.13 Å along the ⟨100⟩, ⟨110⟩, or ⟨111⟩ directions lead to the same minimum value of 9.8% for the R_{wp} factor. In the final step all the atom shifts were simultaneously refined, giving the results presented in Table I.

High-Temperature Phase

The results of the structural refinements performed from the neutron diffraction data collected on the D2B diffractometer between 800 and 307 K are given in Table I. They are in good agreement with those obtained by X-ray diffraction. The reliability

TABLE I

RESULTS OF THE POWDER NEUTRON DIFFRACTION REFINEMENTS OF PMN AT HIGH TEMPERATURE

T(K):	307	400	500	600	700	800
Cell parameter						
a (Å)	4.0500(2)	4.0512(1)	4.0533(2)	4.0570(3)	4.0614(3)	4.0660(4)
Atomic shifts (Å)						
X_{Pb} (Å)	0.337(2)	0.324(2)	0.316(2)	0.310(2)	0.306(2)	0.290(3)
X_{Nb}	0.130(4)	0.137(4)	0.132(4)	0.140(4)	0.135(5)	0.147(4)
$X_{O\parallel}$[a]	0.190(3)	0.196(3)	0.200(3)	0.206(3)	0.211(2)	0.194(2)
$X_{O\perp}$	0.073(4)	0.066(4)	0.064(5)	0.060(6)	0.058(6)	0.053(6)
Isotropic thermal parameters (Å^2) (not refined)						
B_{Pb}	0.68	0.94	1.20	1.47	1.79	2.40
$B_{Mg/Nb}$	0.32	0.39	0.53	0.59	0.76	0.79
B_O	0.49	0.58	0.71	0.82	1.00	1.50
Reliability factors (%)						
R_p[b]	6.12	5.65	5.76	5.88	5.64	5.58
R_{wp}[c]	9.64	9.30	9.32	9.35	8.98	8.97
R_B[d]	2.65	2.47	2.55	2.52	2.57	2.83
R_{exp}[e]	4.14	4.16	4.17	4.19	4.22	4.24

[a] $X_{O\parallel}$: oxygen shifts in the planes parallel to the faces of the cube. $X_{O\perp}$: oxygen shifts along the directions perpendicular to the faces.

[b] Profile $R_p = 100 \times \Sigma(Y_{obs} - Y_{calc})/\Sigma Y_{obs}$.

[c] Weighted profile $R_{wp} = 100 \times \{[\Sigma w(Y_{obs} - Y_{calc})^2/(\Sigma w Y_{obs}^2)]\}^{1/2}$.

[d] Bragg $R_B = 100 \times \Sigma(I_{obs} - I_{calc})/\Sigma I_{obs}$.

[e] Expected $R_{exp} = 100 \times [(N - P)/\Sigma w(Y_{obs})^2]^{1/2}$. I_{obs}, I_{calc}, observed and calculated integrated intensities; w, weight allocated to each data point; N, number of profile points; P, number of parameters.

factors seem to be quite correct: R_{wp}, which is the minimized factor, increases from 8.97 to 9.64% with decreasing temperature and R_B is about 2.6%. The fit between observed and calculated diffraction profiles is satisfactory. The shifts of Pb atoms along the ⟨110⟩ (or ⟨111⟩) directions are 0.29 Å at 800 K and increase up to 0.34 Å at 307 K. The Nb/Mg atom shifts are about 0.13 Å in the whole temperature range and seem to be isotropic. For the oxygen atoms, the shifts are isotropic and remain close to 0.20 Å in planes parallel to the faces of the cube. In the perpendicular direction the shifts are close to 0.06 Å. At 307 K the B–O lengths deduced from these shifts are between 2.20 and 1.86 Å. It is noteworthy that the B site of the perovskite is occupied by Nb^{5+} or Mg^{2+} cations which are chemically different: taking into account their ionic radii (respectively 0.64 and 0.72 Å according to Shannon and Prewitt (*14*)) and their difference in electronegativity (respectively 1.6 and 1.2 in the Pauling scale (*15*)), the Nb–O bonds are expected to be shorter than the Mg–O ones and especially the Nb–O bonds which share their oxygen atom with a Mg^{2+} cation (*16*). So, the evaluated Nb–O bond lengths seem to be quite correct. For the Pb–O bonds, the lengths are between 2.32 and 3.40 Å, which may be compared to the Pb–O bonds of the tetragonal $PbTiO_3$; this oxide exhibits four short Pb–O bonds of 2.52 Å, four bonds of 2.80 Å and four bonds of 3.22 Å. This important anisotropy in the Pb–O bond lengths is originated by the ex-

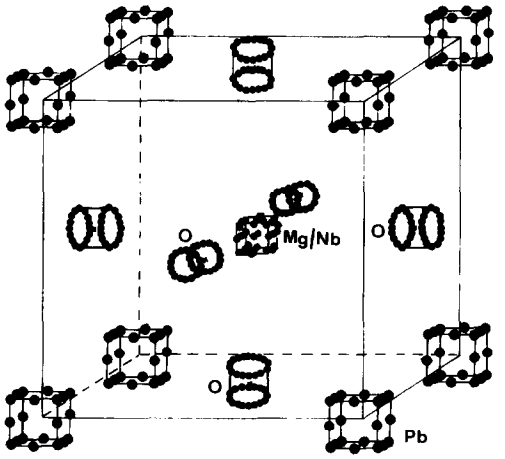

FIG. 6. Disordered cubic structure of the PMN in the paraelectric phase.

istence of a lone pair on the Pb^{2+} cations, which tends to promote a tetragonal pyramidal geometry.

Therefore the chosen structural model seems to be quite correct. The disordered structure of the high temperature phase is presented in Fig. 6 where atomic displacements are magnified by a factor 1.5. This model is very close to that proposed by Itoh *et al.* (*13*) for the cubic phase of $BaTiO_3$: atomic shifts of the *A* and *O* atoms of the perovskite are greater in PMN than in $BaTiO_3$ and the oxygen atoms lie in two planes parallel to the faces of the cube in the PMN instead of remaining within the faces for $BaTiO_3$. This might be due to the existence in PMN of two cations of different nature instead of one on the B site of the perovskite.

Low-Temperature Phase

Considering the absence in the diffraction patterns of splitting or shoulder characteristic of the ferroelectric phase, the previous cubic model has been used in a first step. The refinement results from the X-ray diffraction data are given in Table II. The Pb atom shifts and the reliability factors increase when the temperature decreases. The evolution of the Nb atom shifts versus temperature is irregular. For the refinement of the structure from the neutron diffraction data collected on the D1A diffractometer between 307 and 5 K, the results are given in Table III. The main features are:

(i) At 307 K the R_{wp} factor is lower than that obtained with data recorded on the D2B diffractometer, which has better resolution. This is noticeable at the bases of the lines as is shown in Fig. 4.

(ii) From 307 to 5 K the *R* factors continuously increase, revealing that the disordered cubic model becomes less and less satisfactory.

(iii) The shifts of Pb and O atoms increase slightly when the temperature decreases.

(iv) The shifts of the Nb/Mg atoms are very small and become not detectable at low temperature.

We have then investigated other different structural models, particularly a multiaxial rhombohedral structure of space group *R*3*m*. With such a model, the following results at 5 K have been obtained:

TABLE II

RESULTS OF THE POWDER X-RAY DIFFRACTION REFINEMENTS OF PMN AT LOW TEMPERATURE (CUBIC *Pm3m* STRUCTURE)

T(K):	5	83	240	295
Cell parameter				
a (Å)	4.0499(2)	4.0499(2)	4.0501(2)	4.0501(2)
Atomic shifts (Å)				
X_{Pb} (Å)	0.366(2)	0.362(1)	0.343(1)	0.334(1)
X_{Nb} (Å)	0.220(3)	0.203(1)	0.175(1)	0.220(1)
Isotropic thermal parameters (Å²) (not refined)				
B_{Pb}	0.33	0.42	0.60	0.67
$B_{Mg/Nb}$	0.15	0.19	0.29	0.31
B_O	0.24	0.30	0.44	0.47
Reliability factors (%)				
R_p	11.79	9.05	9.45	8.69
R_{wp}	15.6	11.70	12.01	11.27
R_B	5.28	2.46	1.23	1.77
R_{exp}	4.08	4.66	4.76	4.13

TABLE III

RESULTS OF THE POWDER NEUTRON DIFFRACTION REFINEMENTS OF PMN AT LOW TEMPERATURE (CUBIC *Pm3m* STRUCTURE)

T(K):	5	80	120	200	295	307
Cell parameter						
a (Å)	4.0499(2)	4.0499(2)	4.0495(2)	4.0501(2)	4.0500(2)	4.0500(2)
Atomic shifts (Å)						
X_{Pb}	0.347(1)	0.346(1)	0.344(1)	0.337(1)	0.326(2)	0.329(1)
X_{Nb}	0.003(58)	0.001(19)	0.027(13)	0.066(5)	0.067(5)	0.077(2)
$X_{O\parallel}$	0.185(2)	0.181(2)	0.181(2)	0.171(2)	0.170(2)	0.177(1)
$X_{O\perp}$	0.070(4)	0.069(4)	0.071(4)	0.082(3)	0.079(4)	0.076(4)
Isotropic thermal parameters (Å^2) (not refined)						
B_{Pb}	0.33	0.42	0.46	0.56	0.67	0.69
$B_{Mg/Nb}$	0.15	0.19	0.21	0.26	0.31	0.33
B_O	0.24	0.30	0.33	0.40	0.47	0.48
Reliability factors (%)						
R_p	8.05	8.07	7.74	6.92	6.00	5.11
R_{wp}	11.02	10.79	10.51	9.38	8.41	7.23
R_B	3.03	3.17	2.74	2.02	1.99	1.13
R_{exp}	9.84	9.57	9.76	9.82	9.68	9.85

(i) Pb atoms are statistically shifted by about 0.36 Å along the eight $\langle 111 \rangle_c$ directions of the cube and oxygen atoms by about 0.19 Å along the twelve directions $\langle 331 \rangle_c$. The Nb/Mg displacements could not be evaluated.

(ii) The rhombohedral distortion is extremely weak with $\varphi = 89.984 \pm 0.003°$.

(iii) The structure obtained at 5 K is very close to that obtained for the high temperature phase.

(iv) The reliability factors are only slightly improved, since $R_{wp} = 10.72\%$ and $R_B = 2.49\%$ instead of 11.02 and 3.03.

For both models, when comparing the observed and the calculated neutron diffraction profiles, a good fit for the lines with indices of the same parity and a discrepancy for the other lines are observed, especially when their tails are not taken into account as is seen in Fig. 7.

Conclusion

This work has allowed us to follow the evolution of the structure of the PMN over the temperature range 800–5 K. At 800 K, one can assume that only the cubic paraelectric phase is present. The results lead to a disordered structural model: the atoms are shifted from their special positions ac-

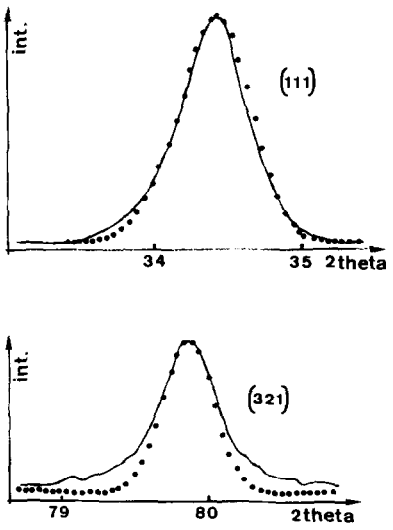

FIG. 7. Observed (full lines) and calculated (points) profiles for the (111) and (321) neutron diffraction lines.

cording to the structural model proposed by Comes *et al.* (*17*) for perovskite oxides and recently illustrated by Itoh *et al.* (*13*) for the cubic $BaTiO_3$ structure.

The appearance of micropolar regions begins at about 600 K, far above the temperature of the maximum of the dielectric constant (270 K). This result is evidenced by:

—The evolution of the thermal expansion coefficient with temperature and the dilatometric studies.

—The appearance of tails at the basis of some Bragg peaks.

The results are in good agreement with the studies of Burns *et al.* (*18*) who report measurements of the temperature dependence of the refractive index and show that from 600 K and below, a local randomly oriented polarization exists in the PMN.

As the temperature is lowered, the local polarized regions spread out and (or) grow; but their correlation lengths are very small even at 5 K and in a first approximation the average structure is roughly cubic. However, the disordered cubic model and the very close multiaxial rhombohedral model lead to R_{wp} factors around 11% at 5 K; the displacements of the Nb/Mg cations could not be accurately evaluated and the profiles of the lines corresponding to reflections with indices of different parities are badly fitted with such models. The line tails observed are due to correlations in the displacements of atoms, originating the polar microregions. The structure factors, for an ideal cubic *Pm3m* perovskite, as a function of the atomic diffusion factors, are:

$$F_{eee} = f_{Pb} + 3f_O + f_{Mg/Nb}$$
$$F_{ooo} = f_{Pb} + 3f_O - f_{Mg/Nb}$$
$$F_{eeo} = f_{Pb} - f_O - f_{Mg/Nb}$$
$$F_{eoo} = f_{Pb} - f_O + f_{Mg/Nb} \qquad e = \text{even};\ o = \text{odd}$$

The lines which remain practically unchanged in the whole temperature range 800–5 K have a large contribution of the oxygen structure factor whereas the others have rather a large contribution of the cations structure factors. On the other hand, line tails are less important on the X-ray than on the neutron diffraction patterns. So, it can be concluded that the lines most sensitive to the Nb/Mg cations are those corresponding to reflections with indices of different parities. This result explains why it is not possible to evaluate the displacements of these cations accurately, especially at low temperature; when the tails are very pronounced a unique Gaussian profile is not sufficient to fit these lines. To improve the profile refinement and thus the structural model it is necessary to introduce pecular correlations between the atomic displacements yielding the observed profiles of the X-ray and neutron diffraction patterns. Refinement calculations based on such models are now in progress.

References

1. L. A. Shebanov, P. Kaspostins, and J. Zvirgzds, *Ferroelectrics* **56,** 1057 (1984).
2. P. Bonneau, P. Garnier, E. Husson, and A. Morell *Mater. Res. Bull.* **24,** 201 (1989).
3. E. Husson, M. Chubb, and A. Morell. *Mater. Res. Bull.* **23,** 357 (1988).
4. H. M. Rietveld, *J. Appl. Crystallogr.* **2,** 65 (1969).
5. D. B. Wiles and R. A. Young, *J. Appl. Crystallogr.* **14,** 149 (1981).
6. C. N. W. Darlington, *J. Phys. C* **21,** 3851 (1988).
7. Deleted in proof.
8. E. Husson, N. de Mathan, P. Bonneau, and A. Morell, "Euroceramics Vol. 2, Properties of Ceramics. (G. de With, R. A. Terpstra and R. Metselaar, Eds.), p. 360, Elsevier (1989).
9. L. E. Cross, S. J. Jang, and R. E. Newnham, *Ferroelectrics* **23,** 187 (1980).
10. L. E. Cross, *Ferroelectrics* **76,** 241 (1987).
11. R. J. Nelmes, Z. Tun and W. F. Kuhs, Institute Laue Langevin Reports, Grenoble, France, Experiments No. 5-15-266 and 5-15-284 (1986).
12. A. M. Glazer and S. A. Mabud, *Acta Crystallogr. Sect. B* **34,** 1065 (1978).

13. H. ITOH, L. Z. ZENG, E. NAKAMURA, AND N. MISHIMA, *Ferroelectrics* **63,** 29 (1985).
14. R. D. SHANNON AND C. T. PREWITT, *Acta Crystallogr. Sect. B* **25,** 925 (1969).
15. L. PAULING "The Chemical Bond" Cornell University Press, 1967.
16. E. HUSSON, L. ABELLO, AND A. MORELL, *Mater. Res. Bull.* **25,** 539 (1990).
17. R. COMES, M. LAMBERT, AND A. GUINIER, *Acta Crystallogr. Sect. A* **26,** 244 (1970).
18. G. BURNS AND F. H. DACOL, *Ferroelectrics* **52,** 103 (1983).